F-15 FLIGHT FLUTTER TEST PROGRAM

Henry Katz, Francis G. Foppe,
and Daniel T. Grossman

McDonnell Aircraft Company

ABSTRACT

The F-15 flight flutter test program is described. Special emphasis is given to test philosophy, data reduction techniques, and test results. The approach utilized for this program not only provided the data necessary to establish a measure of stability for all important flutter mechanisms at each test point, but also allowed extrapolation of the data to actually define all critical flutter boundaries. Such quantitative information was not only useful to definitively establish the flutter status of the aircraft as it was flown, but also provided a solid foundation for assessing the impact of any future design changes.

INTRODUCTION

With very few exceptions, flight flutter testing has historically been conducted on a rather qualitative basis; that is, the only data obtained were the damping available at the test point being flown, with a possible extrapolation of damping trends of the lower damped modes. There generally was no quantitative indication as to the amount of stability remaining at any given point.

The goal set for the F-15 flight flutter test program was to provide a system which would - accurately, quickly, and with a high degree of visibility - allow extrapolation of the data to actually define critical flutter boundaries, in addition to providing a measure of stability for all the important mechanisms at each test point. This was accomplished by designing the aircraft excitation and instrumentation systems to provide high-quality response data which could be speedily and accurately converted to complete (i.e., concerning all modes of interest) damping and frequency information which - in turn - could be utilized for reliable flutter margin predictions by the methods of Reference 1. The accuracy and reliability of these flight flutter test system data not only permitted the pursuit of a minimum flutter margin design concept (and with it optimum weight - see Reference 2) through inflight verification of actual flutter margins of safety, but also provided a quantitative basis on which to quickly assess the impact of future design changes.

This paper concerns itself primarily with test philosophy, data reduction techniques and systems, and test results. Aircraft systems and test operations are covered in Reference 3.

ABBREVIATIONS AND SYMBOLS

CRT	cathode ray tube
g	structural damping coefficient
H_{pc}	pressure altitude, calibrated
Im	imaginary part of transfer function at frequency ω
KEAS	knots equivalent airspeed
L/H	left-hand side
M	Mach number
NBFM	narrow band frequency modulation
PCM	pulse code modulation
Q	dynamic pressure
Re	real part of transfer function at frequency ω
R/H	right-hand side
T_{AF}	temperature at altitude
T-plot	transmissibility plot
V_E	equivalent airspeed
V_T	true airspeed
μ	ratio of structural mass to aerodynamic mass
ρ_A	density at altitude
ω	frequency
ω_n	natural frequency

APPROACH

The quantitative definition of F-15 flutter boundaries from flight test data was accomplished by means of the Flutter Margin technique of Reference 1. This technique permits reliable prediction of flutter speeds on the basis of subcritical test data. Its application requires knowledge - at every test

point - of damping and frequency of every mode involved in potentially critical flutter mechanisms. This complete damping and frequency information was obtained from a unique data reduction facility operating on the aircraft data provided by the exciter and instrumentation systems described in detail in Reference 3.

The method of Reference 1 assumes that data is obtained at different velocities while maintaining the same aerodynamic center and lift curve slopes. Strictly speaking, it is therefore valid only when Mach number is kept constant. The emphasis in this program was, therefore, to obtain constant Mach number cross sections which could be utilized for extrapolation of the data to projected flutter boundaries. M = 0.80 was selected as one of the primary Mach number cross sections to obtain a high subsonic extrapolation point for reference and for correlation with subsonic analyses and wind tunnel tests. Another primary cross section was taken at M = 1.2, the F-15 sea-level design Mach number. Additional Mach numbers at which cross sections were taken were selected on the basis of analyses, wind tunnel tests, and the early portion of the test program, which was dedicated to determining critical Mach numbers by obtaining test data from 0.73 to 1.5 Mach numbers while maintaining a constant dynamic pressure (442 KEAS). The data obtained at this constant dynamic pressure were then reduced in terms of the Flutter Margin parameter to aid in selecting critical Mach numbers for the various critical flutter mechanisms.

Figure 1 shows Flutter Margin as a function of Mach number for one of the critical flutter mechanisms: antisymmetric boom torsion versus stabilator rotation. Basically, a subsonic and a supersonic level can be observed - with some secondary altitude (or μ) effects. The highest Mach number at which the lower subsonic level occurs is just slightly above M = 0.9. Based on such data, and similar results for other modes, M = .93 and M = 1.1 were selected as additional primary Mach numbers and a cross section with three or more flight test points was taken at these points. Secondary Mach numbers of 0.98, 1.04, and 1.15 (with only two flight test points) were selected to provide intermediate checks at a minimum cost in terms of flights required.

A typical flutter prediction at a critical Mach number is shown in Figure 2. It should be noted that the extrapolation is made on the basis of a parabola through the flight test points and the zero airspeed point. Wind tunnel test data have shown that the actual flutter speed will be offset slightly from the parabolic extrapolation toward a point obtained by a straight-line extrapolation through the inflight test points alone. Thus, when the parabola is convex (curving toward the abcissa), the results will be slightly conservative, and the parabola will be used to establish the flutter boundary. In the case of a concave parabola, the straight-line extrapolation will be more conservative and should therefore receive more consideration.

Although, in its strictest sense, the prediction method is invalid for constant altitude data, secondary extrapolations were made at constant altitudes of 1525 and 10 400 m (5000 and 34 000 ft) by taking advantage of the fact that, once supersonic flow is established, the aerodynamic center and lift curve slope are again quite well behaved. An example of a constant altitude extrapolation is shown in Figure 3.

Figure 4 shows the points at which flight flutter data were taken and also indicates the direction of the extrapolations.

EXCITER SYSTEM

The aircraft exciter system, described in detail in Reference 3, furnishes the known forcing function to which aircraft response can be measured. It has the capability to oscillate either the stabilators or the ailerons. Either set of control surfaces can be excited symmetrically (in-phase) or antisymmetrically (out-of-phase). Excitation can be provided either in the form of sweeps (slowly varying frequency through a given range) or dwells/decays (excitation at a given frequency for a certain short time, followed by an abrupt exciter shut-off).

INSTRUMENTATION SYSTEM

As described in Reference 3, the aircraft instrumentation system consists primarily of strain gages, which provide not only the desired response characteristics but also permit relatively independent measurement of the modes of interest. This is important, since it is desired to separate the response in the various modes, especially when these modes are close to each other in frequency. Figure 5 shows the sensor locations on the aircraft and also denotes the primary degree of freedom to be measured by each.

DATA SYSTEM

The heart of the F-15 flight flutter test system is the data handling system. It reduces the information provided by aircraft instrumentation in response to the forcing function furnished by the aircraft exciter system to several forms useful to the flutter engineer.

The F-15 data system can be divided into two parts:

a. The on-line system, which aids in the assessment of stability at the test point being flown at the time; and

b. The post-flight system, which provides a complete evaluation of all the data available to aid in arriving at damping and Flutter Margin trends so as to establish the flutter safety of the next point(s) to be flown and also to extrapolate to predicted flutter boundaries.

On-Line Data System

This portion of the data system provides real-time information as to the stability of the aircraft at the point(s) being flown. It is schematically represented in Figure 6. As can be seen, it involves a mixture of conventional

displays (strip recorders and Lissajous figures) and less conventional information in the form of digitally computed transmissibility plots.

Strip chart recorders

Thirty-two channels of narrow band frequency modulated (NBFM) data are displayed on four strip chart recorders. These channels present the output of strain gages to describe aircraft response and forcing functions. The channels are arranged so that components of critical flutter mechanisms (for example, boom lateral bending and fin bending) are side-by-side to enable close monitoring for the development of any correlation between these degrees of freedom.

The data displayed on the recorders perform the following functions:

a. Allow observation of any correlation between any two degrees of freedom during acceleration into an unexplored flight regime. Such correlation could indicate the approach to an instability.

b. Permit real-time determination of critical modal frequencies during turbulence excitation.

c. Obtain the damping of modes of interest whenever dwell/decay excitation is utilized.

d. Indicate the frequencies of maximum response during a frequency sweep.

e. Monitor the quality of the forcing function during sweeps.

f. Allow observation of the level of turbulence, to determine if acquisition of excitation response data is feasible.

Lissajous displays

Four Lissajous figures each are displayed on four oscilloscopes. The pairs are chosen to provide maximum information on the stability of potential flutter mechanisms. This is accomplished by "beating" the signals from two gages, e.g. from boom lateral bending and fin bending, against each other. The signal from any of the thirty-two NBFM channels can be selected for either axis of any of the sixteen Lissajous figures. These figures are used to observe the phase and frequency relationship between important modal pairs during acceleration into an unexplored flight regime, and are also used to observe the frequency dependence of amplitude and phase during sweeps.

Transmissibility plots

Transmissibility plots are obtained by normalizing response parameters to a parameter which is a measure of the forcing function, e.g. stabilator hinge moment when the stabilators are oscillated. These plots are computed from digitized aircraft response data and present amplitude and phase information as a function of frequency. Figure 7 shows a typical transmissibility plot.

One real-time transmissibility plot (T-plot) for a selected data channel is displayed on a cathode ray tube (CRT) during a sweep. This plot is used to obtain response information for the critical mode of interest. The information is more accurate than can be obtained from the strip recorders in a real-time environment. A side benefit of the real-time T-plot is the immediate acquisition of corrected flight parameters (equivalent airspeed, Mach number, altitude, etc.), which are also displayed on the CRT.

Hard-copy transmissibility plots for six selected data channels are produced on a Gould plotter within 90 seconds after a sweep. The information from these plots, in conjunction with that already obtained from the real-time T-plot, affords the opportunity to obtain a check on frequency and damping values for most of the modes of interest. The ability to determine resonant frequencies almost immediately permits the selection of accurate dwell frequencies during the flight, thus providing good-quality decay data.

Post Flight Data System

This system involves a complete evaluation of all the data available to arrive at damping and Flutter Margin trends so as to establish the flutter safety of the next test point(s), and also to extrapolate to predicted flutter boundaries. A digital computer is used to extract frequency and damping information by the methods of Reference 4 and to provide the data storage and computational capabilities required for the Flutter Margin calculations and predictions. Figure 8 shows the data flow in this system. As can be seen, there is considerable man/machine interaction.

Extraction of frequency and damping data

After the completion of each test flight, transmissibility plots are generated from the onboard tape for all parameters of interest, nominally 12 per sweep, 6 for each side of the aircraft. Frequency and damping are obtained manually from these transmissibility plots by observing resonant peaks and calculating damping on the basis of bandwidth and/or the slope of the phase shift. This information is combined with frequency and damping data obtained from the dwell/decays and the output generated by the automatic modal extraction technique. (The latter is performed in St. Louis because of the larger computer capacity there.)

In the automatic technique, based on Reference 4, the resonant frequencies are considered to occur when the derivatives of the Argand arc-length reaches a maximum with respect to frequency. These maxima are extracted using a least-squares straight-line-slope testing technique. Plots of the derivative are provided to the flutter engineer by the computer (see Figure 9). It was found that a Hanning smoothing technique, applied to both the transfer function and to the derivative data, substantially reduces the error induced by experimental scatter (turbulence, etc.).

To automatically obtain the damping values from the transfer function, the multi-degree of freedom function is initially separated into single degree of freedom segments. The bandwidth of these segments depends on the frequency

separation of the modes and is not the same for all modes. Damping values are extracted for each of the segments by first fitting a least-squares circle to the transfer function data in the complex plane. Damping values are then calculated for each data point used to define the circle, utilizing the equation $g = -\frac{Im}{Re}\frac{\omega_n^2 - \omega^2}{\omega_n \omega}$. The damping values obtained on the basis of the points farthest from the natural frequency are considered to be the most accurate, since they are least sensitive to any error in the frequency term. Therefore, emphasis is placed on the four points which are farthest from the resonant peak (two on each side). The four damping values are presented, along with the average, in a table included with the derivative plot, Figure 9.

Generally, the automatically extracted modes will fall into three categories: good modes, other physical modes, and fictitious modes. In a "good" mode the four damping values will be very close to each other and the same resonant frequency will be shown in the tabulation, the derivative plot and the original transmissibility plot. For example, on Figure 9 the 18.6 Hz boom lateral bending mode and the 33.8 Hz fin tip roll mode are the only good modes to be extracted from this particular gage.

The second category of modes has the following characteristics:

a. Similarity in damping of the two "lower" points and the two "upper" points, but a difference between the "upper" and "lower" points.

b. Good phase-shift at the resonant frequency.

c. Different resonant frequencies indicated by the tabulation, the derivative plot, and the transmissibility plot.

Such modes are generally physical, i.e. real, modes of the airplane, but this particular gage is not the best to discern them; they are better picked off from some other sensor. The 9.9, 13.4, 23.5 and 26.7 Hz modes tabulated in Figure 9 fall into this category.

The 35.4, 37.3 and 39.8 Hz modes are fictitious and can be recognized as such by:

a. Unequal damping values within the "low" and "high" points,

b. Low or even negative damping indications not substantiated by derivative and transmissibility plots.

Utilization of frequency and damping data

Frequency and damping data obtained from the various sources are cross-plotted versus altitude and Mach number for each mode of interest to make sure that they are properly tracked. Figure 10 shows a sample plot of frequency and damping versus Mach number at a constant altitude of 1525 m (5000 ft). Two

modes, fin bending and boom lateral bending, are shown for one side of the aircraft, to demonstrate the range of data scatter that can be expected. As can be seen, the frequency and damping information obtained from the various sources is generally quite consistent. However, in some cases, especially for some of the higher damped modes (see the fin-bending mode in Figure 10), there may be some disagreement between the different bits of information. In such cases, the input data are reviewed regarding their relative merit, e.g. the quality of the decay data, the consistency of the automatically extracted data, and the adequacy of the manually obtained data. Based on a judgment of the relative quality of the different pieces of information, a determination is made on the "final" frequency and damping values to be used for this mode and its "reasonableness" is evaluated by reviewing cross-plots versus altitude and Mach number. This "final" information for each side of the aircraft is then entered into computer storage by means of a remote "Execuport" terminal located at the test site. These data can be retrieved either in tabular form or as Gould plots of frequency, damping, and Flutter Margin versus altitude and Mach number.

At this point, the following data are therefore available to the flutter engineer:

a. Plots of frequency and damping versus altitude for each mode of interest at each cross-section Mach number - Figure 11 is an example of such a plot.

b. Plots of frequency and damping versus Mach number for each mode of interest at each constant altitude cross section - see Figure 10 for sample data of this kind.

c. Plots of Flutter Margin versus equivalent airspeed for each modal combination of interest at each cross-section Mach number (this also includes a prediction of the flutter speed based on a parabolic extrapolation) - see Figure 12.

d. Plots of Flutter Margin versus Mach number for each modal pair of interest at each cross-section altitude - see Figure 13.

Constant altitude flutter velocity predictions are then obtained by manually selecting the Mach number from the constant altitude flutter margin plots at which supersonic flow characteristics appear to be established (e.g. M = 1.18 on the plot in Figure 13), and utilizing only test data above that Mach number for the supersonic extrapolation at this altitude.

A cross-plot of all the Flutter Margin predictions is then made for each modal pair of interest (see Figure 14 for an example) and evaluated in terms of minimum flutter margin. It should be noted that, although modes as determined from left-hand and right-hand data were tracked independently, on the F-15 they were close enough to each other that one flutter boundary could be used to represent them both.

RESULTS

The modes to be observed during the F-15 flight flutter test program were selected on the basis of the results of analytical studies, wind tunnel tests, and ground vibration tests. The modes (both symmetrical and antisymmetrical) tracked on this basis were: fin first bending, fin torsion, fin tip roll, stabilator bending, stabilator pitch, boom lateral bending, boom torsion, boom vertical bending, wing first bending, wing second bending, wing first torsion, outer wing torsion, and aileron rotation.

Data obtained for these various modes were then evaluated in terms of damping versus airspeed at 1525 m (5000 ft), damping versus altitude at the cross-section Mach numbers (to extrapolate to the damping value to be expected at sea level), and flutter boundaries on the basis of Flutter Margin of various modal pairs representing potential flutter mechanisms.

Tables I and II summarize the results of these evaluations in terms of minimum predicted flutter margin for the various mechanisms. It can be noted that there are six flutter mechanisms (three symmetric and three antisymmetric) with predicted flutter margins between 15 and 20 percent, substantiating the success of the minimum weight design concept pursued on the F-15.

Based on our experience to date, we feel that predictions can reliably be carried only to a velocity which is no farther from the last test point than about 1.5 times the difference between the first and last inflight test points. On this basis, since our tests were between altitudes of 6100 and 1525 m (20 000 and 5000 ft), flutter velocity predictions showing greater than 25% flutter margin of safety have no specific quantitative values attached to them.

Shapes of flutter boundaries

Shapes of predicted flutter boundaries were generally either in the form of the boundary given in Figure 14, with Mach numbers between 0.9 and 1.1 being critical, or as shown in Figure 15, with the maximum sea-level Mach number being critical.

Application to design changes

The quantitative knowledge of actual flutter margins provides a firm basis on which to assess the impact of prospective design changes. For example, we may want to incorporate an aircraft modification which, according to analysis (which has been substantially verified by correlation with quantitative flight test data) and possibly also wind tunnel tests, lowers the flutter speed of a certain mechanism by 5%. If we have flight test data in hand that show that we now have 25% margin in this mechanism, we not only have considerable confidence that we can go ahead, but we also have no need to go into another involved flight flutter test program.

We have already had several such opportunities to apply the quantitative F-15 flight flutter test data to the evaluation of design changes.

CONCLUDING REMARKS

The flight flutter test procedure used on the F-15 provides not only a demonstration of adequate damping throughout the aircraft flight envelope, but also permits quantitative demonstration of margin of safety. Such quantitative information is not only useful to definitively establish the flutter status of the aircraft as it was flown, but also provides a solid foundation on which to assess the impact of any future design changes.

REFERENCES

1. Zimmerman, N.H., and Weissenburger, J.T.: Prediction of Flutter Onset Speed Based on Flight Flutter Testing at Subcritical Speeds. Journal of Aircraft, Vol. 1, No. 4, 1964.

2. Shelton, J.D., and Tucker, P.B.: Minimum Weight Design of the F-15 Empennage for Flutter. AIAA/ASME 16th Structures Meeting, May 1975.

3. Nash, D.E., Katz, H., and Moody, W.C.: F-15 Flight Flutter Testing: Aircraft Systems and Test Operations. AIAA 1975 Aircraft Systems and Technology Meeting, August 1975.

4. Kennedy, C.C. and Pancu, C.D.P.: Use of Vectors in Vibration Measurement and Analysis. Journal of Aeronautical Sciences, Vol. 14, 1947.

TABLE I
MINIMUM FLUTTER VELOCITY MARGINS FOR SYMMETRIC MECHANISMS

MECHANISM	MARGIN OF SAFETY
FIN BENDING vs BOOM LATERAL BENDING	15%
STABILATOR BENDING vs STABILATOR ROTATION	19%
WING FIRST BENDING vs OUTER WING TORSION	20%
BOOM VERTICAL BENDING vs STABILATOR ROTATION	25%
BOOM LATERAL BENDING vs BOOM TORSION	> 25%
STABILATOR BENDING vs BOOM TORSION	> 25%
STABILATOR ROTATION vs BOOM TORSION	> 25%
FIN BENDING vs FIN TORSION	> 25%
STABILATOR BENDING vs BOOM VERTICAL BENDING	> 25%
BOOM TORSION vs BOOM VERTICAL BENDING	> 25%
FIN TORSION vs FIN TIP ROLL	> 25%
WING FIRST BENDING vs WING FIRST TORSION	> 25%
WING SECOND BENDING vs WING FIRST TORSION	> 25%
WING SECOND BENDING vs OUTER WING TORSION	> 25%

GP75-0710-2

TABLE II
MINIMUM FLUTTER VELOCITY MARGINS FOR ANTI SYMMETRIC MECHANISMS

MECHANISM	MARGIN OF SAFETY
FIN BENDING vs BOOM LATERAL BENDING	16%
STABILATOR ROTATION vs BOOM TORSION	17%
BOOM LATERAL BENDING vs BOOM TORSION	20%
WING FIRST BENDING vs OUTER WING TORSION	25%
STABILATOR BENDING vs BOOM TORSION	> 25%
BOOM VERTICAL BENDING vs STABILATOR ROTATION	> 25%
WING SECOND BENDING vs OUTER WING TORSION	> 25%
STABILATOR BENDING vs STABILATOR ROTATION	> 25%
FIN BENDING vs FIN TORSION	> 25%
STABILATOR BENDING vs BOOM VERTICAL BENDING	> 25%
BOOM TORSION vs BOOM VERTICAL BENDING	> 25%
FIN TORSION vs FIN TIP ROLL	> 25%
WING FIRST BENDING vs WING FIRST TORSION	> 25%
WING SECOND BENDING vs WING FIRST TORSION	> 25%

GP75-0710-1

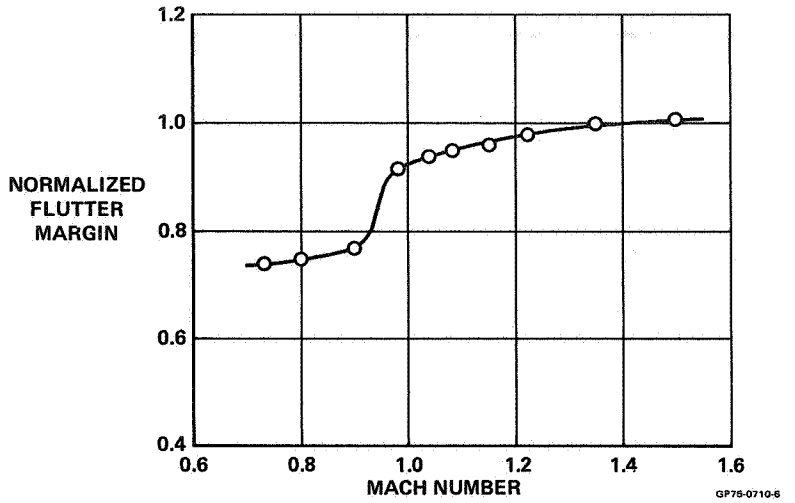

Figure 1.- Flutter margin at constant dynamic pressure. Antisymmetric boom torsion versus stabilator rotation at 442 KEAS.

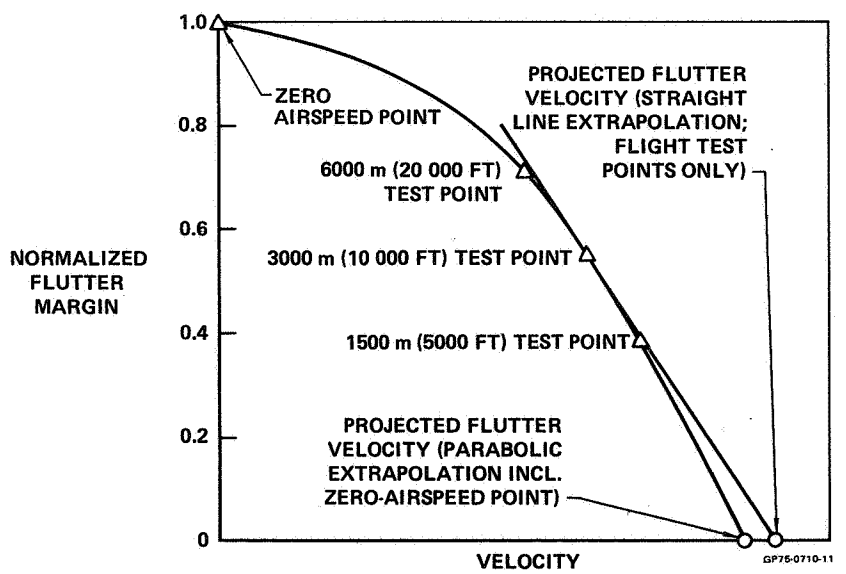

Figure 2.- Flutter prediction at constant Mach number.

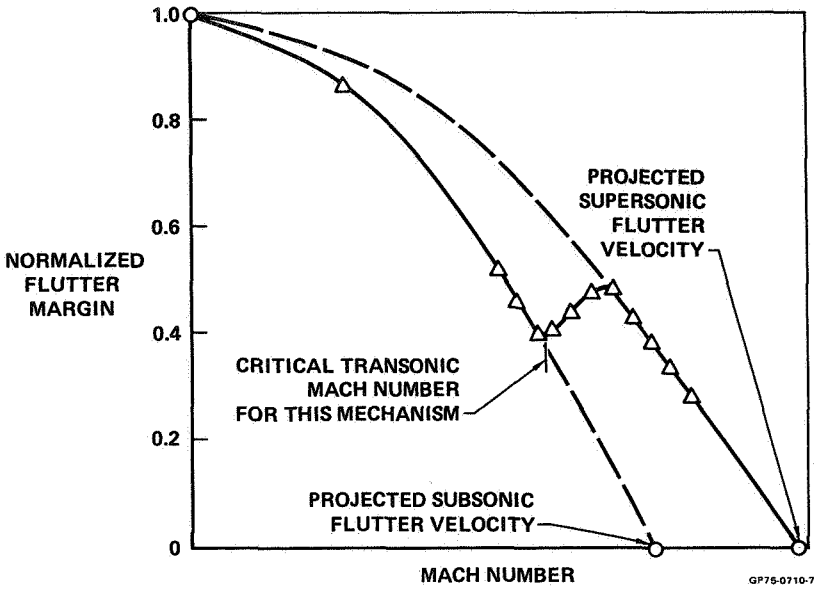

Figure 3.- Flutter prediction at constant altitude.

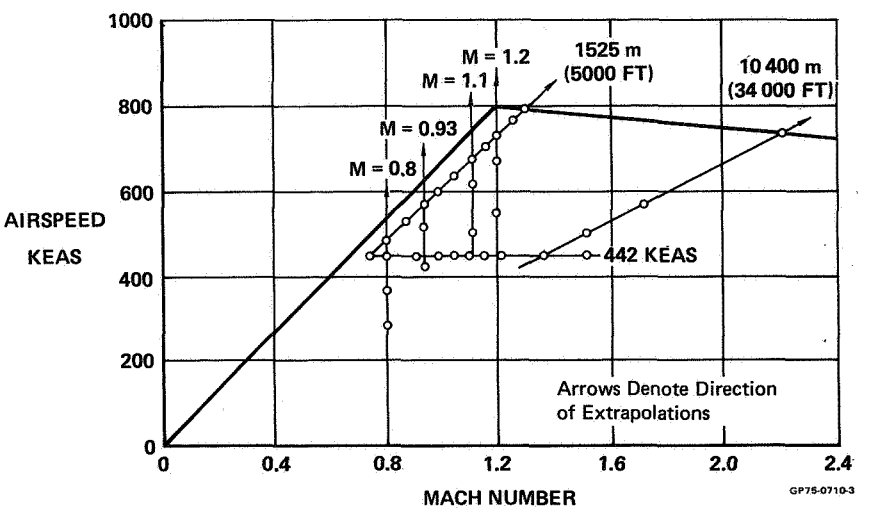

Figure 4.- F-15 flight flutter test points.

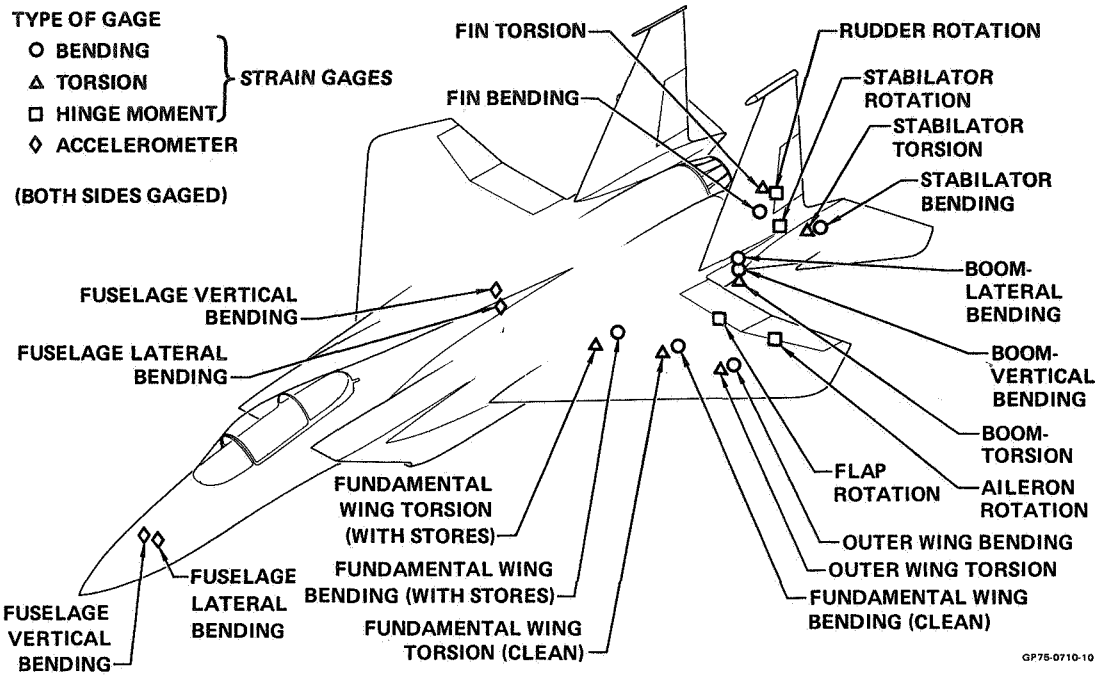

Figure 5.- Location of instrumentation.

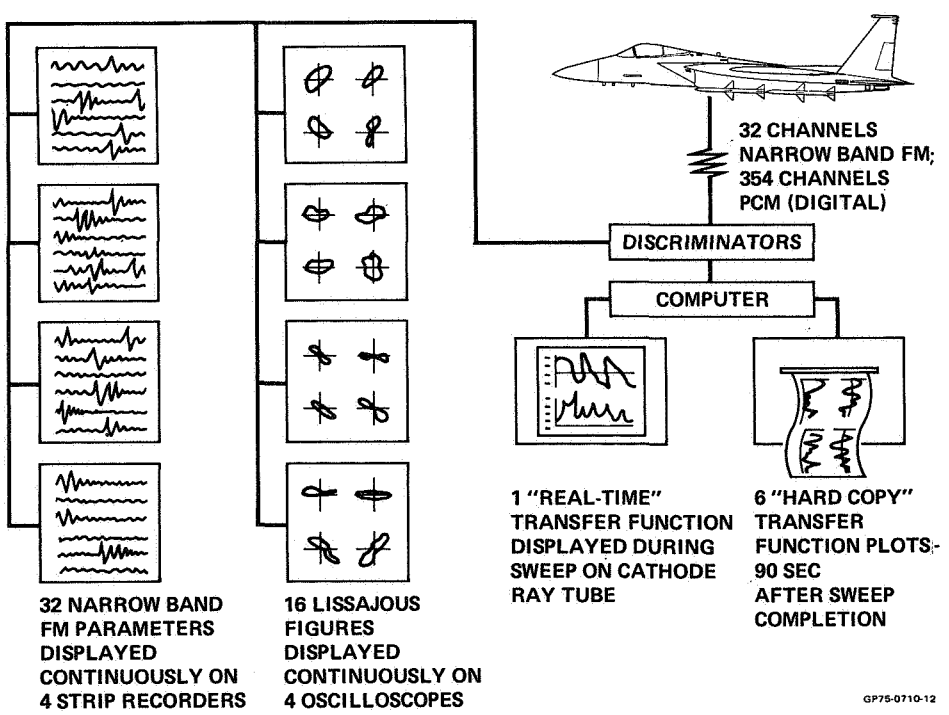

Figure 6.- On-line data reduction of telemetered signals.

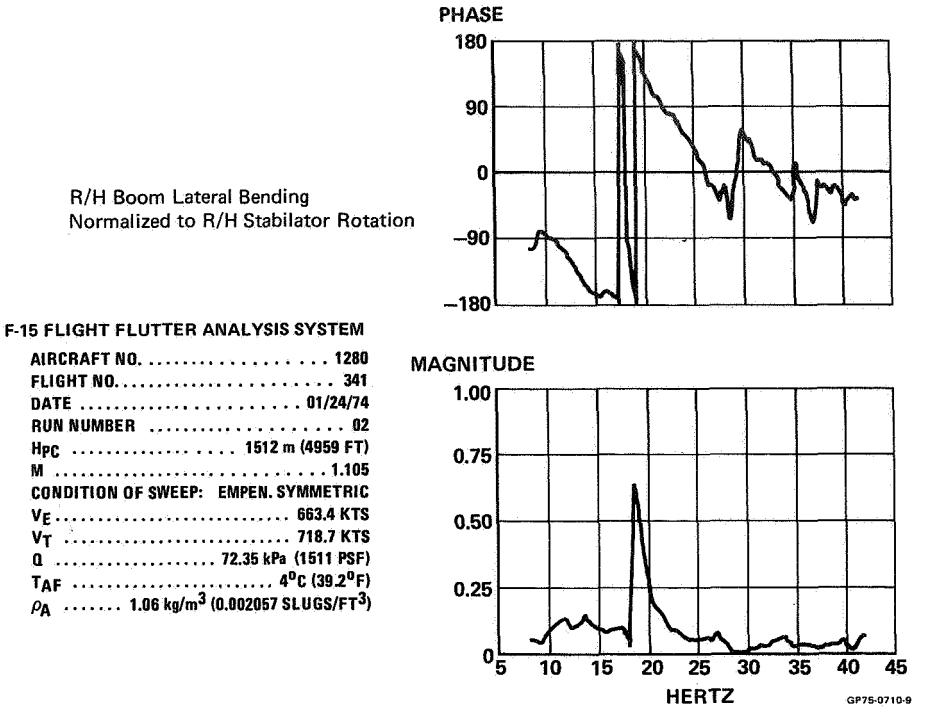

Figure 7.- St. Louis transmissibility plot.

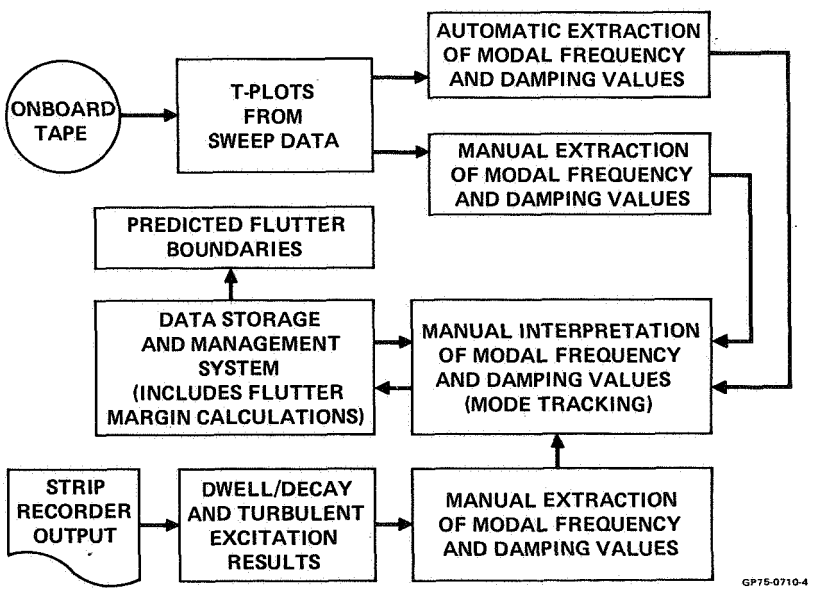

Figure 8.- Post-flight data system schematic.

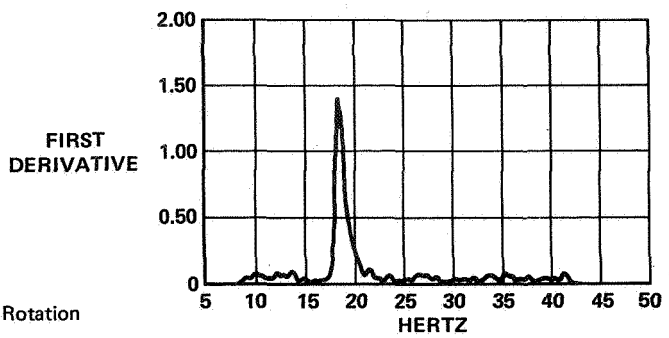

R/H Boom Lateral Bending
Normalized to R/H Stabilator Rotation

F-15 FLIGHT FLUTTER ANALYSIS SYSTEM

AIRCRAFT NO. 1280
FLIGHT NO. 341
DATE 01/24/74
RUN NUMBER 02
H_{PC} . . . . . 1512 m (4959 FT)
M 1.105
CONDITION OF SWEEP: EMPEN. SYMMETRIC
V_E . . . . . 663.4 KTS
V_T . . . . . 718.7 KTS
Q . . . . . 72.35 kPa (1511 PSF)
T_{AF} . . . . . 4°C (39.2°F)
ρ_A . . . . . 1.06 kg/m^3 (0.002057 SLUGS/FT^3)

FREQUENCY AND DAMPING DATA

NUM	FREQ	DAMP	DAMP	DAMP	DAMP	AVG DAMP
1	9.90	0.123	0.114	0.169	0.164	0.142
2	13.40	0.038	0.031	0.024	0.024	0.029
3	18.60	0.019	0.018	0.020	0.021	0.019
4	23.50	0.118	0.100	0.272	0.240	0.183
5	26.69	0.005	0.001	0.034	0.033	0.018
6	33.80	0.025	0.026	0.023	0.028	0.026
7	35.40	−0.002	−0.002	0.001	0.001	0.001
8	37.31	0.033	0.027	0.007	0.008	0.019
9	39.80	0.005	−0.008	−0.009	−0.014	0.005
10						
11						
12						

GP75-0710-8

Figure 9.- St. Louis Argand derivative plot and automatic frequency and damping extraction results.

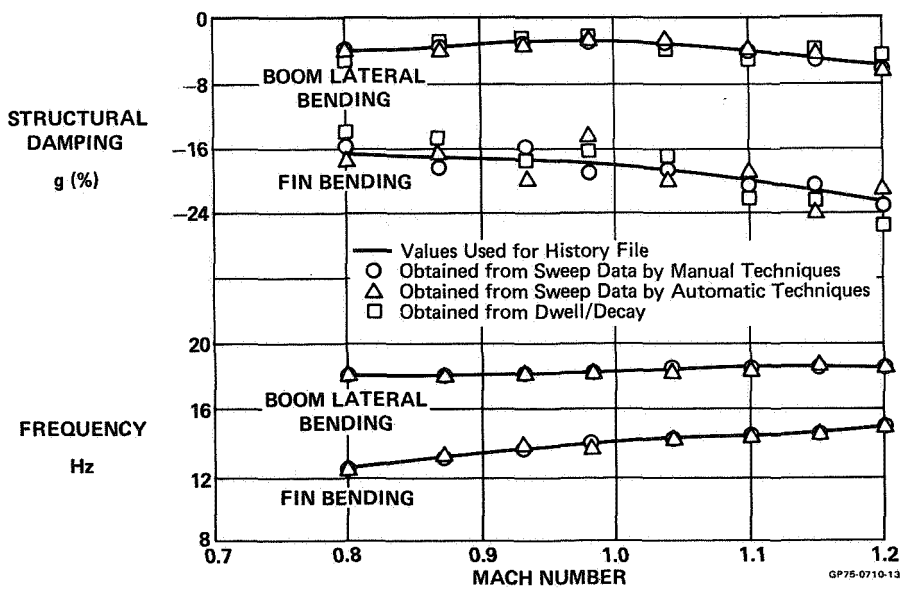

Figure 10.- Frequency and damping versus Mach number for symmetric fin bending and boom lateral bending modes. L/H data at 1525 m (5000 ft) altitude.

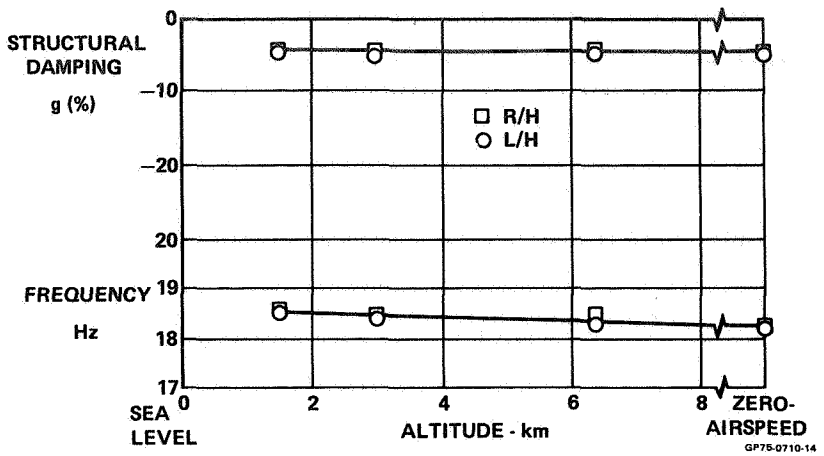

Figure 11.- Frequency and damping versus altitude for symmetric boom lateral bending at constant Mach number of 1.10.

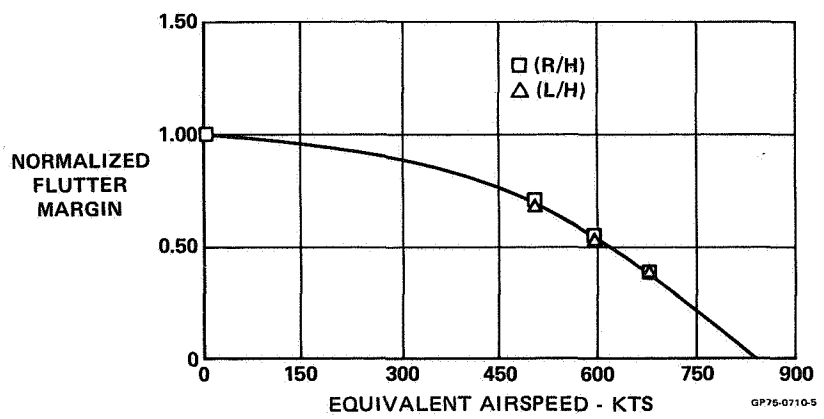

Figure 12.- Flutter margin versus equivalent airspeed. Symmetric boom lateral bending versus fin bending for constant Mach number of 1.10.

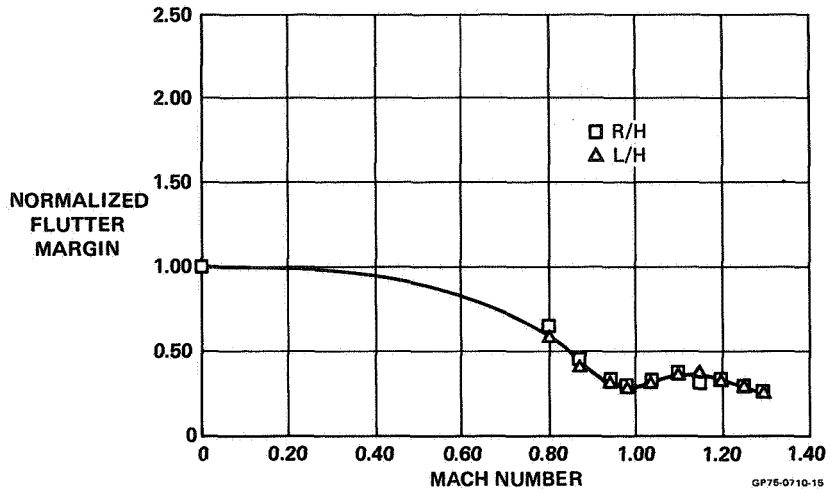

Figure 13.- Flutter margin versus Mach number. Symmetric boom lateral bending versus fin bending at constant altitude of 1525 m (5000 ft).

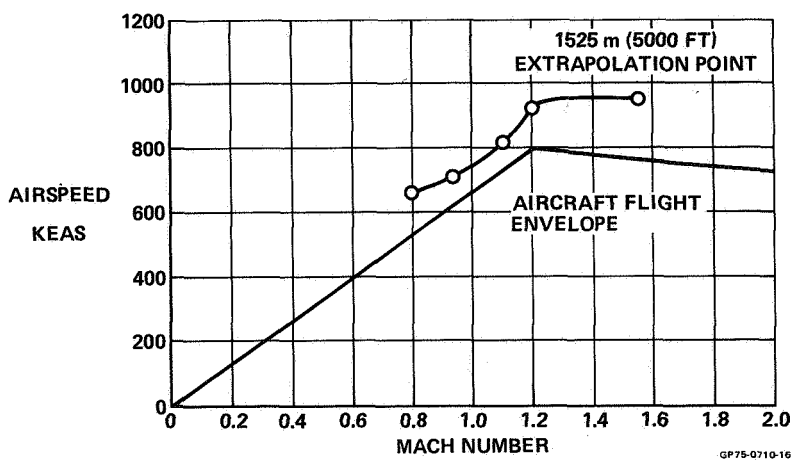

Figure 14.- Flutter boundary for fin bending versus boom lateral bending mechanism - symmetric.

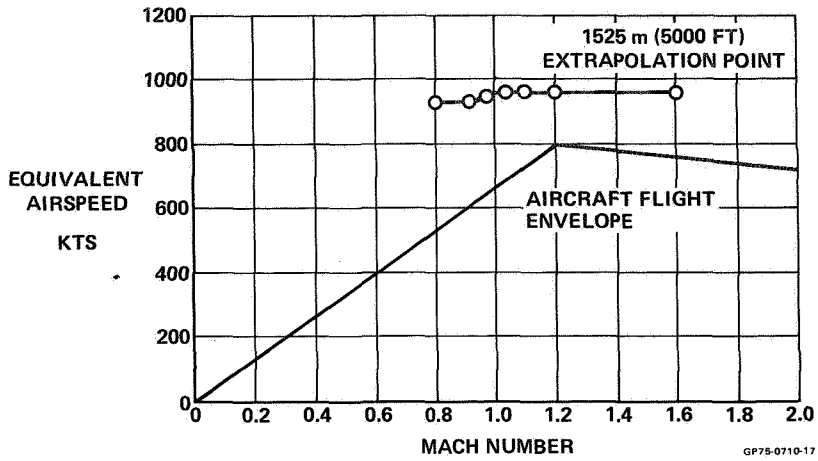

Figure 15.- Flutter boundary for wing first bending versus outer panel torsion mechanism - symmetric.